Free Radical Research, Volume 38 Number 9 (September 2004), pp. 951–962

Taylor & Francis
healthsciences

Ability of Ferric Nitrilotriacetate Complex with Three pH-dependent Conformations to Induce Lipid Peroxidation

KAORI AKAI[a], KOICHIRO TSUCHIYA[a], AKIRA TOKUMURA[a], KENTARO KOGURE[a], SATORU UENO[a], AKIRA SHIBATA[a], TOSHIAKI TAMAKI[b] and KENJI FUKUZAWA[a,*]

[a]*Graduate School of Pharmaceutical Sciences, The University of Tokushima, 1-78-1 Sho-machi, Tokushima 770-8505, Japan;* [b]*Department of Pharmacology, The University of Tokushima School of Medicine, 3-18-15 Kuramoto, Tokushima 770-8503, Japan*

Accepted by Professor E. Niki

(Received 12 March 2004; In revised form 19 June 2004)

This study examined the generation of reactive oxygen species (ROS) and the induction of lipid peroxidation by carcinogenic iron(III)–NTA complex (1:1), which has three conformations with two pKa values ($pKa_1 \approx 4$, $pKa_2 \approx 8$). These conformations are type (a) in acidic conditions of pH 1–6, type (n) in neutral conditions of pH 3–9, and type (b) in basic conditions of pH 7–10. The iron(III)–NTA complex was reduced to iron(II) complex under cool-white fluorescent light without the presence of any reducer. The reduction rates of three species of iron(III)–NTA were in the order type (a) ⩾ type (n) > type (b). Iron(III)–NTA-dependent lipid peroxidation was induced in the presence and absence of preformed lipid peroxides (L-OOH) through processes associated with and without photoreduction of iron(III). The order of the abilities of the three species of iron(III)–NTA to initiate the three mechanisms of lipid peroxidation was: (1) type (a) > type (n) > type (b) in lipid peroxidation that is induced L-OOH- and H_2O_2-dependently and mediated by the photoreduction of iron(III); (2) type (b) > type (n) > type (a) in lipid peroxidation that is induced L-OOH- and H_2O_2-dependently but not mediated by the photoreduction of iron(III); (3) type (n) > type (b) > type (a) in lipid peroxidation that is induced peroxide-independently and mediated by the photoactivation but not by the photoreduction of iron(III). The rate of lipid peroxidation induced L-OOH-dependently is faster than that induced H_2O_2-dependently in the mechanism (1), but the rate of lipid peroxidation induced H_2O_2-dependently is faster than that induced L-OOH-dependently in the mechanism (2). In the lag process of mechanism (3), L-OOH and/or some free radical species, not $^1O_2$, were generated by photoactivation of iron(III)–NTA. These multiple pro-oxidant properties that depend on the species of iron(III)–NTA were postulated to be a principal cause of its carcinogenicity.

Keywords: Lipid peroxidation; Nitrilotriacetate; Free radical; Ferric nitrilotriacetate; Carcinogenesis; Reactive oxygen species

Abbreviations: BP, 2,2′-bipyridyl; DTMA, N-dodecyltrimethylammonium chloride; LH, linoleic acid; L-OOH, linoleic acid hydroperoxide; NTA, nitrilotriacetic acid; $^1O_2$, singlet oxygen; $O_2^{\cdot-}$, superoxide anion radical; $^{\cdot}OH$, hydroxyl radical; ROS, reactive oxygen species; TBA, 2-thiobarbituric acid; TBARS, thiobarbituric acid-reactive substances; TPP, triphenylphosphine

INTRODUCTION

Although iron is an essential element in the living system, its acute or chronic overload sometimes causes toxic effects. Several studies have associated iron poisoning with oxidative damage.[1,2] *In vivo* treatment with the ferric chelate of nitrilotriacetate (NTA), an aminotricarboxylic acid, has been reported to produce severe acute and subacute nephrotoxicity and renal adenocarcinomas in experimental animals.[3–5] Oxidized DNA such as bulky DNA adducts and 8-hydroxydeoxyguanosine were significantly increased in renal tumors[3–5] and excreted urine[6,7] of animals administered iron(III)–NTA. Iron(III)–NTA also increased renal accumulation of lipid aldehydes such as malondialdehyde (MDA) and 4-hydroxy-2-alkenals that are derived from lipid peroxides, in parallel with an increase in protein carbonyl concentrations.[8,9] *In vitro* exposure to iron(III)–NTA complex also induced generation of hydroxyl radicals ($^{\cdot}OH$),[10,11] high lipid peroxidation[12–15] and damage to DNA bases[15,16] and deoxyribose.[12,17] These results suggest that the toxic properties of iron(III)–NTA may be due to its

*Corresponding author. Fax: +81-88-633-9572. E-mail: fukuzawa@ph.tokushima-u.ac.jp

ISSN 1071-5762 print/ISSN 1029-2470 online © 2004 Taylor & Francis Ltd
DOI: 10.1080/1071576042000261945

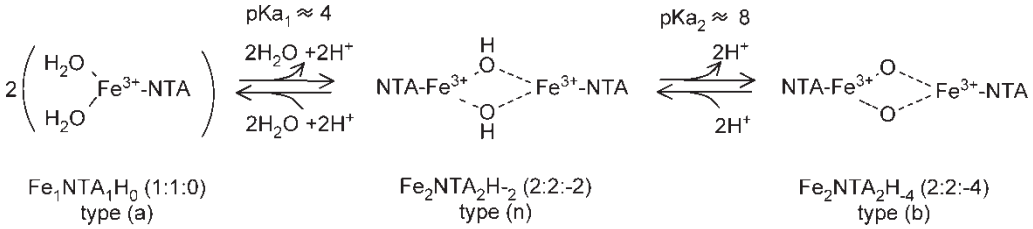

SCHEME 1 pH-dependent conformation changes of iron(III)–NTA complex.

high oxidation potential. This is confirmed by the findings that dietary vitamin E, a known scavenger of free radicals, protects against Fe-NTA-induced nephrotoxicity by inhibiting lipid peroxidation.[4]

An equimolar complex of iron(III)–NTA was reported to form three conformations dependent on pH, that is, type (a) in acidic conditions of pH 1–6, type (n) in neutral conditions of pH 3–9, and type (b) in basic conditions of pH 7–10.[18] As shown in Scheme 1, type (a) has a monomeric structure coordinated with H_2O [(1:1:0) species], type (n) has a dimeric structure with μ-hydroxyl-bridges to iron(III) [(2:2:-2) species], which is formed by dehydration and deprotonation of type (a), and further deprotonation of a OH-bridge of type (n) makes type (b), which has a dimeric structure with μ-oxo-bridges to iron(III) [(2:2:-4) species]. Recently, Gabricevic and Crumbliss[19] reported that their pKa values were 4.36 and 7.58. There is every likelihood that three types of the iron(III)–NTA complex are present in urine because of its wide pH range from 4.6 to 7.5. It is important for clarification of carcinogenisity of iron(III)–NTA complex to investigate which species of iron(III)–NTA complex is the powerful oxidant.

It has been widely believed that an effective oxidant of iron complex is the ferrous type, because it generates powerful oxidant species. As candidates for the *in vivo* reducer of iron(III)–NTA complex, NADPH-cytochrome p450 reductase,[14,20] oxyhemoglobin in circulation,[21] superoxide anion radical ($O_2^{\cdot-}$) produced by xanthine − xanthine oxidase[14,22] and endogenous thiol compounds[8,23] have been proposed. On the other hand, the evidence that iron(III)–NTA complex produces 5,5-dimethyl-1-pyrroline-N-oxide (DMPO) spin adducts in the absence of a reducer[24] suggests that iron(III)–NTA complex generates reactive oxygen species (ROS) without reducer. Furthermore, iron(III)–NTA complex plus H_2O_2 has also been reported to form $^{\cdot}OH$ (at pH 7.4)[25] or $O_2^{\cdot-}$ (at pH 10)[26] without reducer.

Since iron(III)–NTA is known to be reduced by photoirradiation,[27] we used photo-chemical reduction of iron(III)–NTA complex in this study, because it can be used in acidic and basic conditions, while the enzymatic reduction cannot. Furthermore, photo-chemical reduction was preferable because it does not function like chemical reducers, which not only reduce iron(III)–NTA complex but may also affect other redox-related reactions.

In this study, to elucidate the mechanisms of how iron(III)–NTA complex initiate lipid peroxidation, we investigated the pH-dependent photo-chemical reduction of three species of iron(III)–NTA and their ability for pH-dependent initiation of lipid peroxidation under photo-irradiated and -intercepted conditions. We further investigated the effect of the presence of hydroperoxides such as H_2O_2 and lipid peroxides on iron(III)–NTA-dependent lipid peroxidation, because peroxides are usually required in generation of radical oxidants for initiation of lipid peroxidation.

MATERIALS AND METHODS

Materials

Linoleic acid (LH), 2,2′-bipyridine (BP), butylhydroxytoluene (BHT), 2-thiobarbituric acid (TBA), triphenylphosphine (TPP), and $Fe(NO_3)_3{\cdot}9H_2O$ were obtained from Wako Pure Chemical Industries (Tokyo, Japan). Sodium nitrilotriacetate (NTA-2Na), diethylenetriamine pentaacetic acid (DTPA) and $Fe(NH_4)_2(SO_4)_2{\cdot}6H_2O$ were from Nacalai Tesque Inc. (Kyoto, Japan). N-dodecyltrimethylammonium chloride (DTMA) and 1,1,3,3-tetraethoxypropane (TEP) were purchased from Tokyo Chemical Industries (Tokyo, Japan). β-Carotene was purchased from Sigma Chemical Co. (St Louis USA). α-Tocopherol was kindly provided by Eisai Co. (Tokyo, Japan). All other reagents were of analytical grade. Water processed with a Milli-Q system (Millipore, Milford, MA, USA) was used to prepare all reagents.

Preparation of Iron(III)–NTA Solution

Stock solutions of $Fe(NO_3)_3{\cdot}9H_2O$ (0.1 M) and NTA-2Na (0.1 M) were prepared on the day of measurement. The iron-NTA complex was prepared by adding appropriate amount of iron and NTA from stock solutions at acidic pH (< pH 2) to distilled water before use, and kept in darkness.

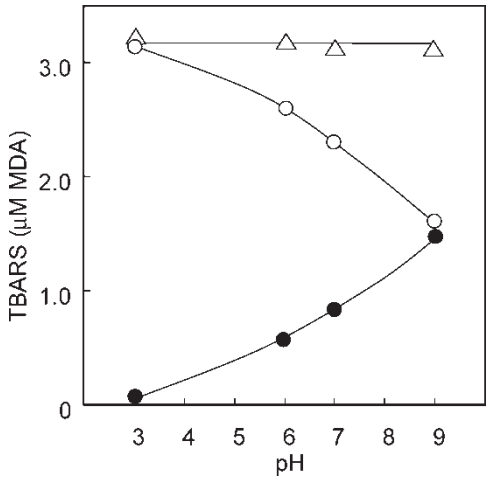

FIGURE 1 The pH-dependency of the rate of iron(III)–NTA-induced TBARS formation in LH micelles under photo-irradiated and photo-intercepted conditions. (Δ) photo-irradiated condition; (●) photo-intercepted condition; (○) difference between photo-irradiated and photo-intercepted values. Each values were obtained after subtraction of the values without incubation from those incubated for 60 min. Concentrations of reagents were: 5 mM linoleic acid containing 10 μM L-OOH, 50 mM DTMA and 0.2 mM iron(III)–NTA (1:1). The pH was adjusted with HCl or NaOH. The irradiation condition was 92 μW/cm^2 (UV-A) or 12 μW/cm^2 (UV-B). Incubation was carried out at 25°C for 60 min.

Preparation of LH Micelles

LH was dispersed in the form of mixed micelles with DTMA. A solution of LH in chloroform was placed in a test tube, and the solvent was evaporated under nitrogen. When necessary, α-tocopherol or β-carotene was added to the chloroform solution of LH. The lipid film of 25 μmol LH was dissolved in 5 ml of 50 mM DTMA solution, vortexed and sonicated in a Bransonic-12 sonic bath (Yamato Tokyo, Japan).[13] The concentration of linoleic acid hydroperoxides (L-OOH) contamination in LH was determined by the xylenol orange method.[28] The commercial LH sample was contaminated with 0.2 mol% of L-OOH. When necessary, L-OOH contamination was reduced by treatment of the LH with TPP in chloroform solution just before preparation of micelles.

Photoirradiation

Photoirradiation conditions were 92 μW/cm^2 (UV-A) and 12 μW/cm^2 (UV-B) in Fig. 1, 3 μW/cm^2 (UV-A) and 1 μW/cm^2 (UV-B) in Fig. 2, and 720 μW/cm^2 (UV-A) and 75 μW/cm^2 (UV-B) in Figs. 3–7. The photo intensity was monitored using UV-radiometer UVR-3036/S (Topcon Tokyo, Japan).

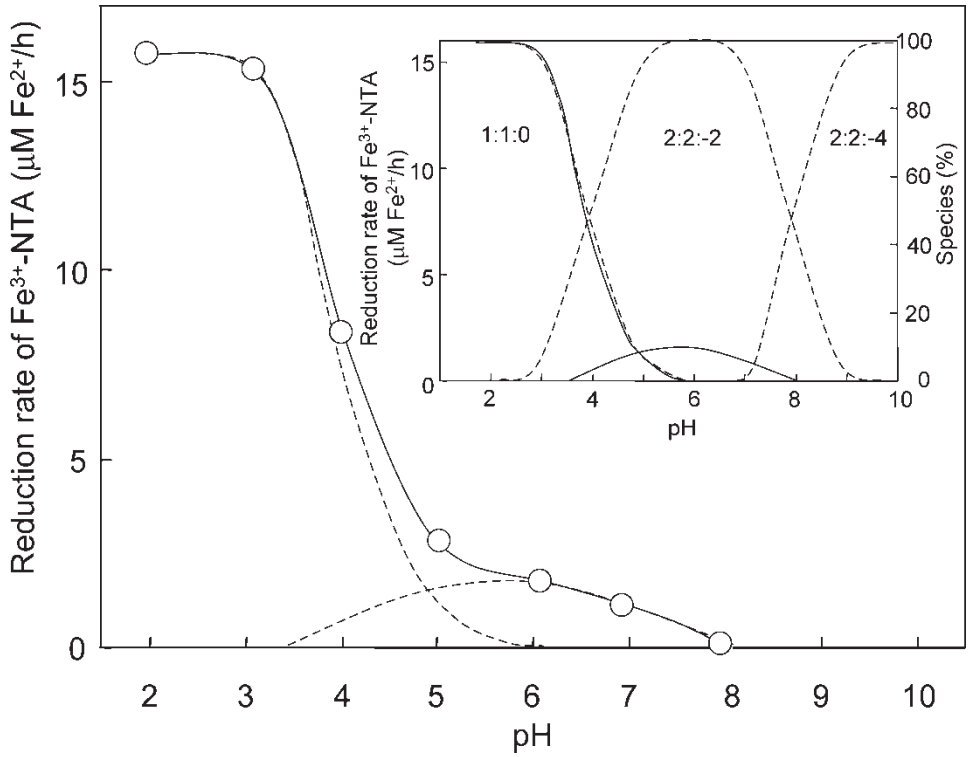

FIGURE 2 The pH-dependency of the photoreduction rate of iron(III)–NTA to iron(II)–NTA under anaerobic condition. Concentrations of irradiated reagents were 0.75 mM iron(III)–NTA (1:1) and 15 mM KCl. The pH was adjusted with HCl or NaOH. Irradiation condition was 3 μW/cm^2 (UV-A) and 1 μW/cm^2 (UV-B). A curve plotted experimentally (solid line with white symbols) was separated by curve-fitting analysis into two components (broken lines). The inset shows the pH-dependencies of the curve-fitting analyzed reduction rates of iron(III)–NTA (solid lines) and the fractional diagrams of iron(III)–NTA species (broken lines), which refer to Ogasawara and Yokoi.[18]

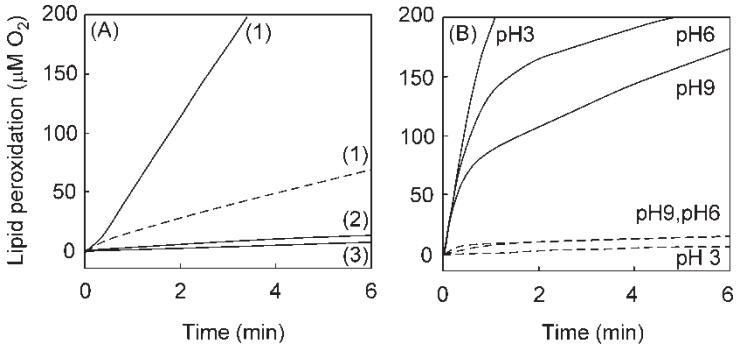

FIGURE 3 The iron(III)–NTA-and iron(II)–NTA-induced oxygen consumption indicative of peroxidation of LH with and without TPP pretreatment under photo-irradiated and photo-intercepted conditions. The photoirradiation condition was 720 μW/cm^2 (UV-A) and 75 μW/cm^2 (UV-B). Incubation was carried out at 37°C. (A) Iron(III)–NTA system. (1) Complete system, (2) NTA was omitted from complete system, (3) iron(III) was omitted from complete system. Solid and broken lines indicate photo-irradiated and photo-intercepted conditions, respectively. Concentrations of reagents in complete system were: 5 mM linoleic acid containing 10 μM L-OOH, 50 mM DTMA and 0.2 mM iron(III)–NTA. Incubation was carried out at pH 6. The reaction was started by the addition of iron(III)–NTA. (B) Iron(II)–NTA system. Linoleic acid with (broken lines) or without (solid lines) TPP pretreatment was incubated with iron(II)–NTA at pH 3, pH 6, and pH 9 under the photo-intercepted condition. Concentrations of reagents were: 5 mM linoleic acid containing 10 μM L-OOH, 50 mM DTMA and 20 μM iron(II)–NTA. Linoleic acid (5 mM) was pretreated with and without 50 μM TPP. The reaction was started by the addition of iron(II). Iron(II)–NTA was completely oxidized 2 min after its addition.

Assays of Lipid Peroxidation

Lipid peroxidation of LH micelles was measured by following the consumption of oxygen and formation of TBA-reactive substances (TBARS). The typical reaction system consisted of 5 mM LH, 50 mM DTMA and 0.2 mM iron(III)–NTA. The rate of oxygen consumption associated with lipid peroxidation was measured with a Clark-type oxygen electrode, assuming an oxygen concentration of 217 μM in the initial incubation mixture at 37°C.[14] When necessary, to intercept the light, a cell of oxygen electrode was covered with aluminum foil. The pH was adjusted with HCl or NaOH. The TBA method was used as described previously.[29] The oxidation was started by the addition of 20 μl of iron(III)–NTA to 2 ml of LH micelles and stopped by the addition of 400 μl of 40 mM DTPA, followed by 2 ml of 3 M acetate buffer (pH 3.5), 100 μl of an ethanol solution of 1.6% BHT, and 1 ml of an aqueous solution of 0.67% TBA. The mixture was heated at 95°C for 30 min, cooled with tap water, and mixed with 4 ml of *n*-butanol, and the absorbance in *n*-butanol was measured at 535 nm. The amount of TBARS formed was expressed as equivalents of MDA. The TEP was used as an external standard for the quantitation of MDA. Other experimental details are described in the figure legends.

Reduction Rate of Iron(III)–NTA to Iron(II)–NTA

The amount of iron(II)–NTA formed by the photochemical reduction of iron(III)–NTA was determined from the amount of iron(II)–BP complex formed by the reaction of BP with iron(II)–NTA.[30] Irradiation mixture contained 0.75 mM iron(III)–NTA (1:1) and 15 mM KCl, which was vigorously purged with argon for 20 min before preparation of the mixture. After irradiation at 25°C under an anaerobic condition, 2 ml of reaction mixture was added to 1 ml of 30 mM BP (final concentrations were 0.5 mM iron(III)–NTA, 10 mM BP and 10 mM KCl), and the absorption of iron(II)–$(BP)_3$ formed was measured at 520 nm. The amount of iron(II)–$(BP)_3$ was determined using the molar absorption coefficient at 520 nm ($\varepsilon = 8,600\,M^{-1}cm^{-1}$).[31] The concentrations of iron(II)–(BP) were plotted versus time, and the reduction rate was calculated from the slope of the line using a computer.

Recording of Voltammograms of Iron(III)–NTA

Differential pulse voltammograms were recorded with a YANACO P-1100 polarographic analyzer (Yanagimoto Co., Tokyo) with a platinum plate (30 × 5 mm) electrode, platinum wire counter electrode, and saturated calomel electrode (SCE) reference electrode. All scans were done at room temperature and at scan rates of 10 mV/s. Volumes of 15 ml of 10 mM KCl solution at various pH values were placed in the cell, and the voltammograms recorded as blanks. Then, an aliquot of 5 mM iron(III)–NTA (1:1) in 10 mM KCl solution was added, and the voltammogram curve was recorded with mechanical stirring. During the measurements, nitrogen was passed over the surface of the solution.

RESULTS

Lipid Peroxidation Induced by Iron(III)–NTA under Photo-irradiated and Photo-intercepted Conditions at Various pH Values

We and other researchers have reported that iron(III)–NTA complex causes lipid peroxidation

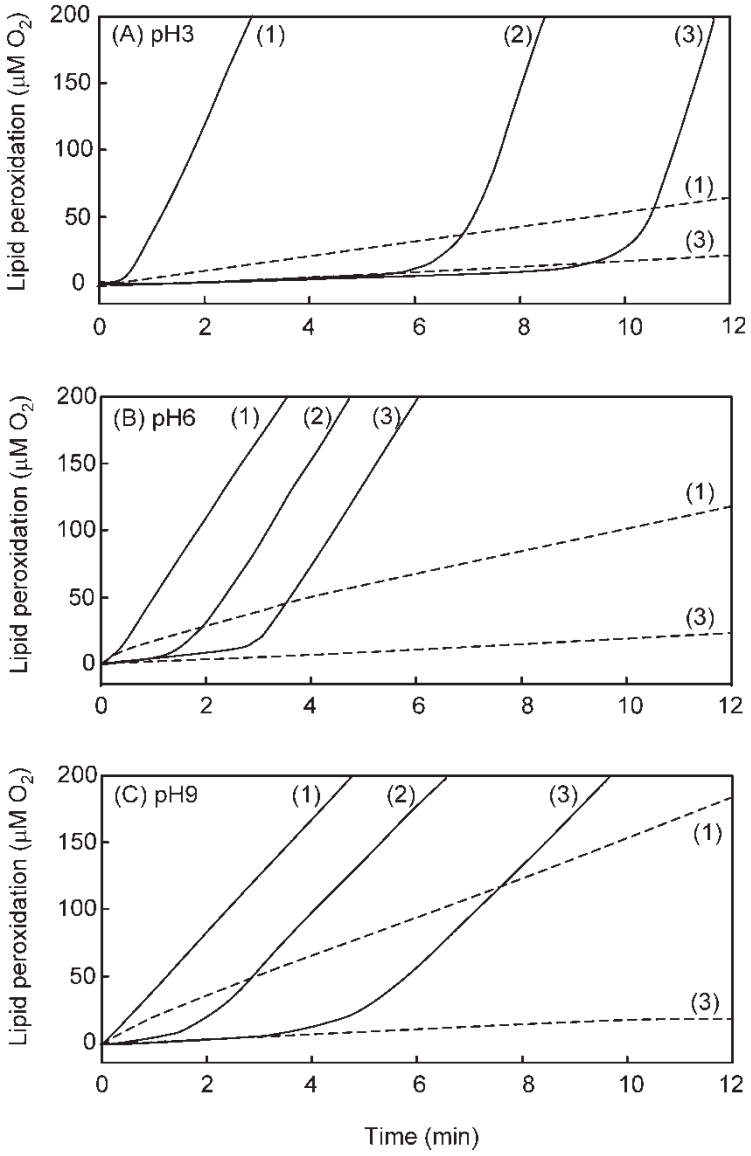

FIGURE 4 Time courses of the iron(III)–NTA-induced peroxidation of linoleic acid with and without TPP pretreatment under photo-irradiated and photo-intercepted conditions at various pH. (1) Linoleic acid (5 mM) was not pretreated with TPP, (2) linoleic acid (5 mM) was pretreated with 20 μM TPP, (3) linoleic acid (5 mM) was pretreated with 50 μM TPP. Solid and broken lines indicate photo-irradiated and photo-intercepted conditions, respectively. Experimental conditions were as shown in Fig. 3. The real rates of lipid peroxidation under photo-irradiated condition, which were obtained after subtraction of the values measured under photo-intercepted conditions (broken lines (1)) from the values measured under photo-irradiated conditions (solid (1)), were 85.2, 49.3, and 34.5 μM/min at pH 3, pH 6, and pH 9, respectively.

both *in vitro* and *in vivo*.[12–15] However, although iron(III)–NTA is known to be reduced by photo-irradiation,[27] no attention has been paid to the effect of room light on these experiments. Therefore, we studied the effect of room light on iron(III)–NTA-dependent lipid peroxidation. Furthermore, since iron(III)–NTA is known to form three pH-dependent conformations,[18] we investigated the effect of pH on lipid peroxidation to determine which species of iron(III)–NTA complex is the effective initiator. As shown in Fig. 1, the rate of TBARS formation in DTMA micelles of LH incubated with iron(III)–NTA complex under room light was almost the same at any pH studied here. No TBARS were produced at pH 3, and the rate of TBARS formation under the photo-intercepted condition increased with increasing pH. On the other hand, the difference in the TBARS formation rate between photo-irradiated and photo-intercepted conditions, indicative of photo-dependent lipid peroxidation, was decreased with increasing pH.

pH Dependency of the Rate of Photo-chemical Reduction of Iron(III)–NTA Complex

The photo-irradiated reduction of iron(III)–NTA was investigated by measuring the absorption spectra of iron(II)–BP complex. Absorbance of iron(II)–$(BP)_3$

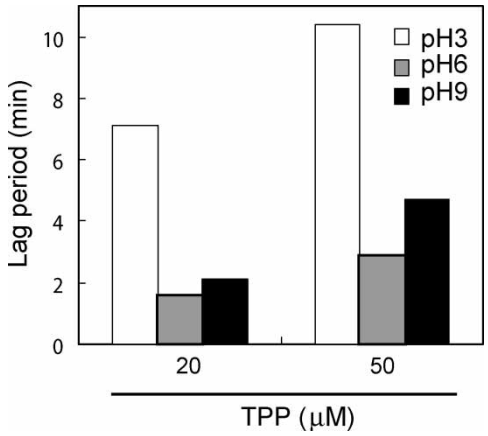

FIGURE 5 The effect of TPP concentration on lag period of the iron(III)–NTA-induced lipid peroxidation at pH 3, 6, and 9 under the photo-irradiated condition. Data were obtained from Fig. 4(A)–(C) (solid lines (1)–(3)).

complex at 520 nm was gradually produced at the time of irradiation. Figure 2 shows the pH-dependency of the rate of photo-chemical reduction of iron(III)–NTA complex under an anaerobic condition, which could be divided into two components, (indicated by broken lines in Fig. 2). These profiles were completely dependent on the fractional diagram of iron(III)–NTA complex (inset in Fig. 2) reported by Ogasawara *et al.*[18] Judging from these results and from the conformation of the equimolar complex dependent on pH (Scheme 1), it was expected that the monomeric structure [(1:1:0) species] and the dimeric structure with μ-hydroxyl-bridges to iron(III) [(2:2:-2) species] would be susceptible to photoreduction but the dimeric structure with μ-oxo-bridges to iron(III) [(2:2:-4) species] would not.

Reduction Potentials of Iron(III)–NTA

To obtain the reduction potential of iron(III)–NTA, we measured the differential pulse voltammograms of iron(III)–NTA in KCl solution at various pH. The values of reduction potentials were +0.04 V (pH 3), −0.24 V (pH 6) and −0.40 V (pH 9), which are well reflected in their easiness to be photo-reduced (Fig. 2).

Photo-dependent and -independent Lipid Peroxidation Induced by Iron(III)- and Iron(II)–NTA with Three Conformations in the Presence and Absence of Preformed Lipid Peroxides

As shown in Fig. 3(A), oxygen indicative of lipid peroxidation was rapidly consumed in the complete system containing LH of DTMA micelles and iron(III)–NTA at pH 6. The rate of oxygen consumption of complete system under photo-irradiated condition was faster than that under photo-intercepted condition. Little oxygen consumption was observed when iron(III) or NTA was omitted from complete system.

Ferrous iron is known to catalyze lipid peroxidation by generating powerful oxidant species such as hydroxyl and lipid alkoxyl radicals by the Fenton reaction. As the rapid oxygen consumption under photo-irradiated condition was supposed to be attributable to the photo-reduced iron(II)–NTA complex, we investigated the initiation effect of iron(II)–NTA on lipid peroxidation under photo-intercepted condition. As was expected, even under the photo-intercepted condition, iron(II)–NTA exhibited a very rapid oxygen consumption and then relatively slow oxygen consumption followed in the presence of L-OOH (solid lines in Fig. 3(B)). The oxygen consumption of the latter is possibly caused by the reaction of oxidized iron(III)–NTA with endogenous L-OOH, because their rates at pH 6 and 9 were the same as the rates of iron(III)–NTA system (broken lines (1) in Fig. 4(B) and (C) shown later). However, when LH was pretreated with TPP, which reduces endogenous L-OOH to the corresponding alcohol (L-OH),[32] oxygen was slightly consumed by iron(II)–NTA under the photo-intercepted condition (broken lines in Fig. 3(B)).

Lines (1) in Fig. 4(A)–(C) show the pH-dependency of the rate of iron(III)–NTA-dependent oxygen consumption in micelles of LH without TPP-pretreatment. The order of the rates was pH 3 > pH 6 > pH 9 under the photo-irradiated condition (solid lines (1)) and pH 9 > pH 6 > pH 3 under the photo-intercepted condition (broken lines (1)). These results are very consistent with the results of Fig. 1.

Under the photo-intercepted condition, no oxygen consumption occurred at any pH value in the system of LH pretreated with TPP (broken lines (3) in Fig. 4), indicating that the photo-independent lipid peroxidation was L-OOH-dependently induced by iron-(III)–NTA. But under the photo-irradiated condition, rapid oxygen consumption occurred after a time lag in TPP-pretreated LH micelles (solid lines of (2) and (3) in Fig. 4(A)–(C)). The rates of rapid oxygen consumption after lag period in micelles of LH pretreated with TPP (solid lines of (2) and (3)) were almost the same as that in micelles of LH without TPP pretreatment (solid lines of (1)) in either pH conditions. However, the lag time increased with the increase in the concentration of pretreated TPP, that changed pH dependently. The length of the lag period was in the order pH 3 > pH 9 > pH 6 (Fig. 5). The surplus TPP would be consumed by the L-OOH and/or some radicals generated by photo-activated iron(III)–NTA during the lag period in the order pH 6 > pH 9 > pH 3, and after TPP disappeared, rapid lipid peroxidation was induced L-OOH-dependently.

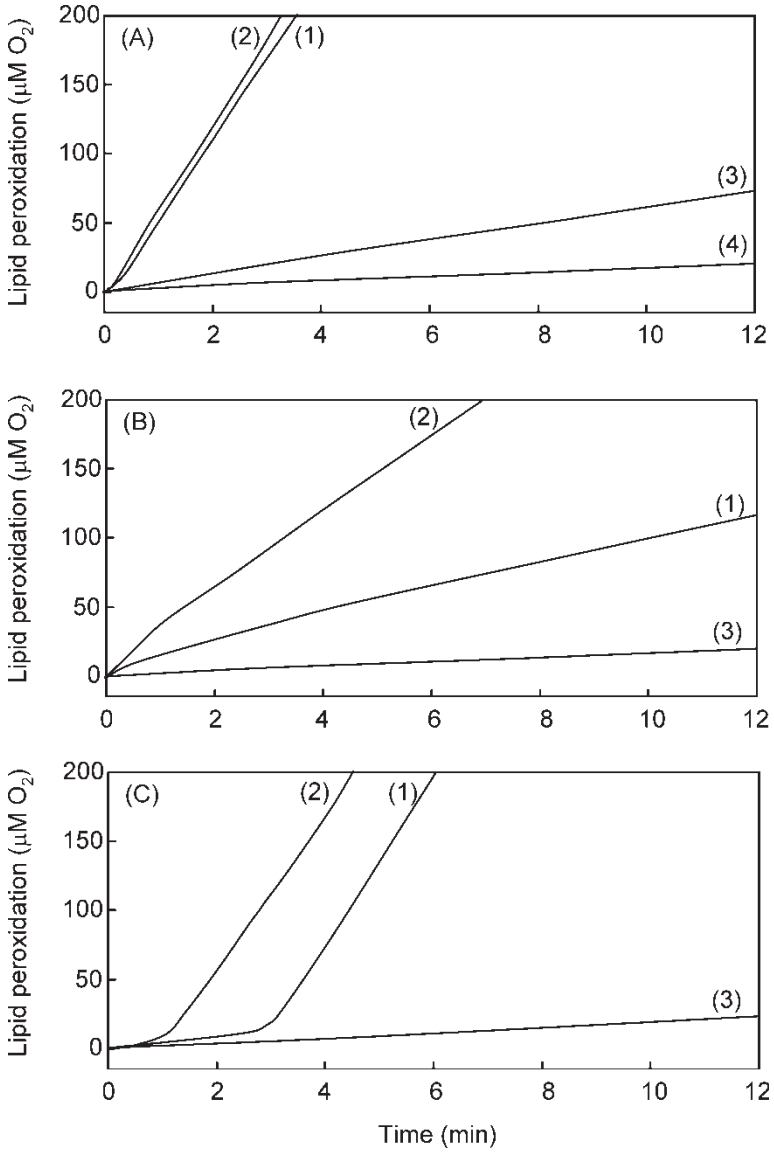

FIGURE 6 The effect of β-carotene and α-tocopherol on the iron(III)–NTA-induced peroxidation of linoleic acid with and without TPP pretreatment under photo-irradiated and photo-intercepted conditions. (A) The rate of lipid peroxidation under photoirradiation condition. Linoleic acid was not pretreated with TPP. (B) The rate of lipid peroxidation under photo-intercepted condition. Linoleic acid was not pretreated with TPP. (C) The rate of lipid peroxidation under photoirradiation condition. Linoleic acid was pretreated with 50 μM TPP. (1) none (control), (2) β-carotene (50 μM), (3) α-tocopherol (10 μM), (4) α-tocopherol (50 μM). Incubation was carried out at pH 6. Other experimental conditions are as shown in Fig. 3.

The Effect of β-carotene and α-tocopherol on the Iron(III)–NTA-dependent Lipid Peroxidation

To elucidate the mechanism of what active oxygen species are generated by photoirradiation during the lag period, we investigated the effect of α-tocopherol, a well-known radical scavenger, and β-carotene, a well-known singlet oxygen ($^1O_2$) scavenger on the iron(III)–NTA-induced lipid peroxidation. As shown in Fig. 6, under photo-irradiated and photo-intercepted conditions, α-tocopherol inhibited lipid peroxidation but β-carotene did not inhibit lipid peroxidation and shortened the lag period. These results indicate that some free-radicals, but not $^1O_2$, participate in the initiation processes of the lipid peroxidation.

H_2O_2-dependent Lipid Peroxidation Induced by Iron(III)–NTA under Photo-irradiated and Photo-intercepted Conditions

We recently observed that iron(III)–NTA complex generated H_2O_2 and $^{\cdot}OH$ under photo-irradiated conditions (manuscript in preparation). Accordingly, we investigated the effect of catalase on iron(III)–NTA-dependent lipid peroxidation. Addition of catalase (1000 IU/ml) showed a slight inhibition of lipid peroxidation at pH 6 under photo-irradiated condition (data not shown), indicating that H_2O_2 contributes a little to the photo-induced iron(III)–NTA-dependent lipid peroxidation. We further studied the effect of H_2O_2 externally added on

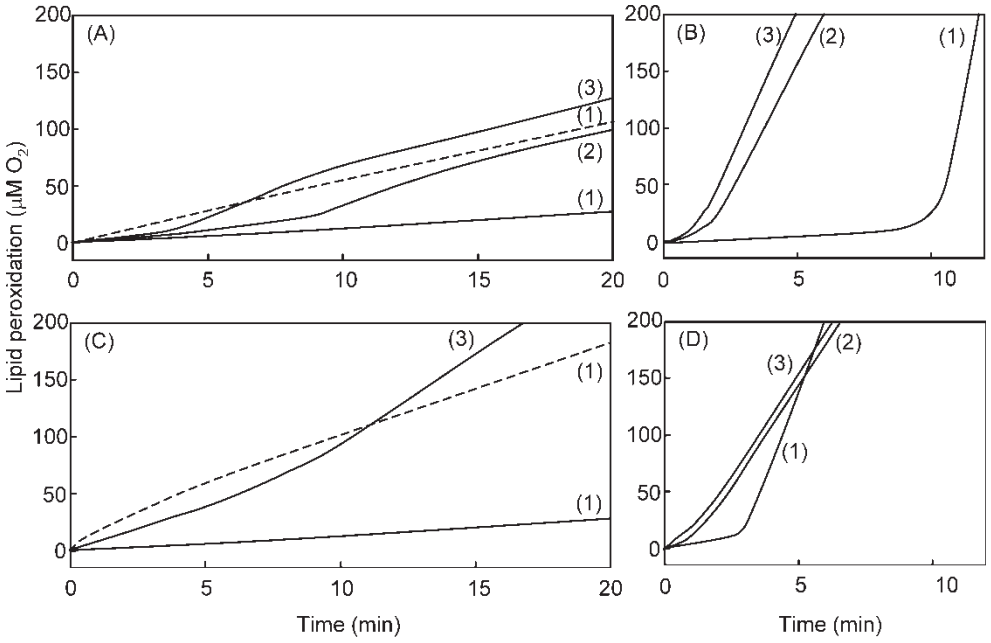

FIGURE 7 The iron(III)–NTA-induced peroxidation of linoleic acid with TPP pretreatment in the presence of H_2O_2 at pH 3 and 6 under photo-irradiated and photo-intercepted conditions. Reaction mixtures containing 5 mM linoleic acid pretreated with or without 50 μM TPP, 50 mM DTMA and 0.2 mM iron(III)–NTA were incubated in the presence of 100 or 200 μM H_2O_2. (1) none (control), (2) 100 μM H_2O_2, (3) 200 μM H_2O_2. Solid lines: linoleic acid (5 mM) was pretreated with 50 μM TPP; broken lines: linoleic acid (5 mM) was not pretreated with TPP. (A) The rate of lipid peroxidation at pH 3 under photo-intercepted condition. (B) The rate of lipid peroxidation at pH 3 under photoirradiation condition. (C) The rate of lipid peroxidation at pH 6 under photo-intercepted condition. (D) The rate of lipid peroxidation at pH 6 under photoirradiation condition. The incubation and photoirradiation conditions are as shown in Fig. 3.

iron(III)–NTA-induced lipid peroxidation at pH 3 and 6 (examination was not done at pH 9 because of instability of H_2O_2). As shown in Fig. 7, lipid peroxidation was induced by the addition of H_2O_2 in the absence of L-OOH in TPP-pretreated LH either under photo-irradiated or photo-intercepted condition. The oxygen consumption rates were higher under the photo-irradiated condition (Fig. 7(B) and (D)) than under photo-intercepted condition (Fig. 7(A) and (C)). Under photo-intercepted condition at pH 3 (Fig. 7(A)), lipid peroxidation in the system of TPP pretreated was not induced in the absence of H_2O_2 (solid line (1)) but induced after a time lag in the presence of H_2O_2 (solid lines (2) and (3)). The length of the lag period decreased with the increase in the concentration of H_2O_2 added. The progress of oxygen consumption after a time lag was two steps, faster rate at first followed by a slower rate (a solid line (3) in Fig. 7(A) is typical), and the rate of the latter (solid lines (2) and (3)) was the same as the rate of TPP-untreated system (broken line (1)). We supposed that after the surplus TPP was consumed by the H_2O_2 added and $^{\cdot}OH$ formed from it by the reaction with iron(III)–NTA during lag period, H_2O_2-dependent faster lipid peroxidation started, and then the L-OOH-dependent slower lipid peroxidation followed after H_2O_2 disappeared.

Similar results were observed at pH 6 (Fig. 7(C)). The oxygen consumption rates during and immediately after a time lag were higher at pH 6 (Fig. 7(C)) than at pH 3 (Fig. 7(A)), indicating that the ability of iron(III)–NTA for initiation of H_2O_2-dependent lipid peroxidation was: (2:2:-2) > (1:1:0).

The rates of photo-induced oxygen consumption after a time lag in the presence and absence of H_2O_2 were shown in Fig. 7(B) and (D). The rates of lines (2) and (3) after a time lag which were induced by photo-irradiated iron(III)–NTA dependently on H_2O_2, were higher at pH 3 than at pH 6. These rates (lines (2) and (3)) were slower than those of lines (1), which would be induced by photo-irradiated iron(III)–NTA dependently on L-OOH formed during lag period, at either pH 3 or 6, indicating that photo-reduced iron(II)–NTA induced more rapidly L-OOH-dependent lipid peroxidation than H_2O_2-dependent lipid peroxidation.

DISCUSSION

We investigated the mechanism of lipid peroxidation induced by carcinogenic iron(III)–NTA which has three pH-dependent conformations. Oxygen consumption indicative of iron(III)–NTA-dependent lipid peroxidation was more facilitated in the photo-irradiated condition than in the photo-intercepted condition at any pH value (Fig. 4). The results obtained by measuring oxygen consumption correlated well with those obtained by measuring TBARS formation (Fig. 1). The orders of the facilitation by

iron(III)–NTA were as follows: (1:1:0) > (2:2:-2) > (2:2:-4) in photo-dependent lipid peroxidation, and (2:2:-4) > (2:2:-2) > (1:1:0) in photo-independent lipid peroxidation (Fig. 4). These results suggest that there are atleast two mechanisms for initiation of lipid peroxidation by iron(III)–NTA, photo-dependent and photo-independent mechanisms. Furthermore, as mentioned below, the former mechanism has two processes: one includes the photoreduction of iron(III)–NTA to iron(II)–NTA complex, which facilitates the lipid peroxidation, as iron(II)–NTA does, and the other does not.

We previously reported that iron(II)–NTA induced oxidation of LH micelles in the presence of L-OOH by the following equations.[13]

$$\text{L–OOH} + \text{iron(II)–NTA} \rightarrow \text{L–O}^{\cdot} + \text{iron(III)–NTA} + \text{OH}^{-}$$

$$\text{L–O}^{\cdot} + \text{LH} \rightarrow \text{L–OH} + \text{L}^{\cdot} \quad \text{(initiation reaction)}$$

Pretreatment with TPP, which is known to reduce L-OOH to L-OH, attenuated these reactions.[13,33] Therefore, we investigated the effect of TPP pretreatment on iron(III)–NTA-dependent lipid peroxidation. Under the photo-intercepted condition, no oxygen consumption occurred in TPP-pretreated LH micelles, but under the photo-irradiated condition, oxygen consumption occurred after a lag period. The pH-dependent profile of the photoreduction rate of iron(III)–NTA complex, which showed rapid photoreduction of (1:1:0) species, slow photoreduction of (2:2:-2) species and no photoreduction of (2:2:-4) species (Fig. 2), suggests that the (1:1:0) and (2:2:-2) species induce L-OOH-dependent lipid peroxidation mediated by photoreduction in acid and neutral conditions, respectively, but (2:2:-4) species does not in alkaline condition.

The rate of L-OOH-dependent lipid peroxidation under photo-intercepted condition was in the order pH 9 > pH 6 > pH 3 (Fig. 4). This order was in proportion to the order of their reduction potentials, suggesting that iron(III)–NTA gives the initiators such as L-O$^{\cdot}$ by the reductive cleavage of L-OOH.

The time lag increased with the increase in the concentration of the TPP pretreatment (Fig. 5). We conjectured that the surplus TPP used to reduce L-OOH is consumed during lag period by photo-irradiated iron(III)–NTA, and then the apparent oxygen consumption induced was dependent on L-OOH. These results suggest that induction of photo-dependent lipid peroxidation by iron(III)–NTA was L-OOH-dependent and -independent, but photo-independent lipid peroxidation was induced only L-OOH-dependently.

Photo-dependent and -independent lipid peroxidations were also induced by iron(III)–NTA in the presence of H_2O_2 instead of L-OOH. In photo-irradiated system, $^{\cdot}$OH generated from H_2O_2 by Fenton reaction with photo-reduced iron(II)–NTA was supposed to be an initiator of the lipid peroxidation. In photo-intercepted system, $^{\cdot}$OH was also suggested to function as an initiator of the lipid peroxidation, because iron(III)–NTA complex plus H_2O_2 was reported to form $^{\cdot}$OH (at pH 7.4) without reducer.[25] The rate of H_2O_2-dependent lipid peroxidation was faster under photo-irradiated condition than under photo-intercepted condition (Fig. 7). The former system would generate $^{\cdot}$OH faster than the latter system does. Under photo-intercepted condition, the oxygen consumption rates during and just after a time lag were higher at pH 6 than at pH 3 (solid lines (3) in Fig. 7(A) and (C)), indicating that the order of the initiation ability of iron(III)–NTA/H_2O_2-dependent lipid peroxidation was: (2:2:-2) > (1:1:0).

The reactions of photosensitizers are divided into two groups: formation of free-radicals (type I reaction) and generation of $^1O_2$ (type II reaction).[34] The type II reaction is unlikely during the lag time because the $^1O_2$ scavenger β-carotene neither inhibited the photo-irradiated lipid peroxidation nor elongated the lag period (Fig. 6). Contrary to expectation, β-carotene showed the pro-oxidant effect (line (3) in Fig. 6(B) and (C)). We did not give a reason for pro-oxidant effect of β-carotene but supposed it may act as a initiator of lipid peroxidation, because Niki[35] reported the possibility that β-caroteneperoxyl radical, which is formed by the reaction of β-carotene with peroxyl radical, attacks lipids and abstracts hydrogen to induce the chain reaction.

It is also unlikely that H_2O_2 generated through auto-oxidation of reduced iron(III)–NTA during the lag period is a main initiator, because there were no correlation between the activities of the three iron(III)–NTA species in shortening the lag time (Fig. 5) and their abilities to be photo-reduced from iron(III) to iron(II) (Fig. 2), by which H_2O_2-dependent lipid peroxidation was induced. The photoexcited photosensitizer is well known to abstract an electron from the acceptor substrate.[34] Since a radical scavenger α-tocopherol effectively inhibited the photo-irradiated lipid peroxidation (Fig. 6), we supposed that photo-activated iron(III)–NTA (*Fe^{3+}-NTA in Scheme 2) may directly draw hydrogen from LH to form L$^{\cdot}$, which is scavenged by α-tocopherol. A possibility of non-radical species such as an activated iron oxygen complex being generated still remains, because the inhibitory effect of α-tocopherol might be caused by scavenging L-OO$^{\cdot}$ derived from the activated complex. From the pH-dependency of shortening the lag period in the system with TPP treatment (Fig. 5), the order of type I reaction was: (2:2:-2) > (2:2:-4) > (1:1:0).

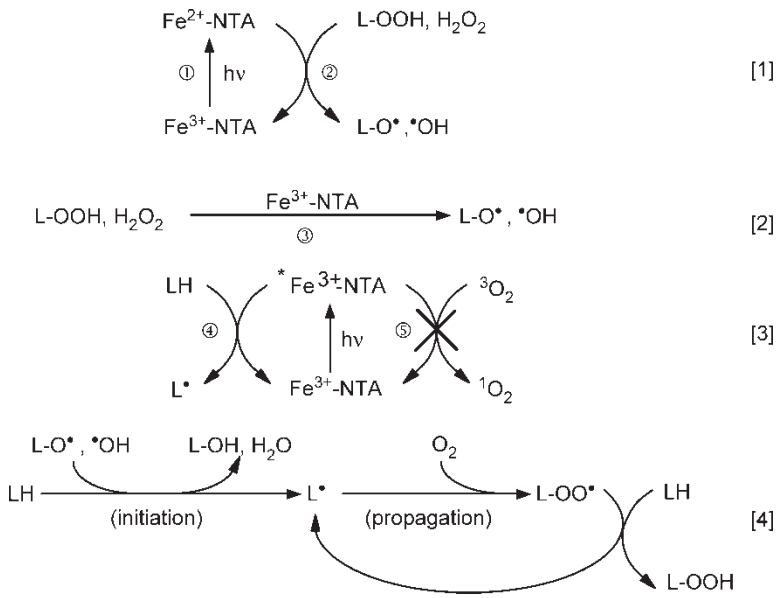

SCHEME 2 Proposed mechanisms for initiation of iron(III)–NTA-dependent lipid peroxidation.

Considering these results, we propose three mechanisms for initiation of iron(III)–NTA-dependent lipid peroxidation as summarized in Scheme 2: (1) photo-reduced iron(II)–NTA reacts with preformed L-OOH and/or the H_2O_2 generated from $O_2^{\cdot-}$ by auto-oxidation of iron(II)–NTA, and forms L-O$^{\cdot}$ and/or $^{\cdot}$OH (Eq. 1), initiators of lipid peroxidation (Eq. 4); (2) iron(III)–NTA reductively cleaves L-OOH and/or H_2O_2 without being reduced to iron(II)–NTA, and forms initiators such as L-O$^{\cdot}$ and/or $^{\cdot}$OH (Eq. 2); or (3) photo-activated iron(III)–NTA draws the hydrogen directly from LH to form L$^{\cdot}$ (Eq. 3), which facilitates the propagation of lipid peroxidation (Eq. 4). The relative abilities of the three species of iron(III)–NTA to catalyze the five reactions in Scheme 2 were summarized in Table I.

The pH-dependent reactions for generation of active oxygen species, which catalyze the initiation step (Eq. 4 in Scheme 2) of the chain reaction of lipid peroxidation, were as follows: at the condition of pH 9, a reaction ③ only progressed under photo-intercepted

TABLE I Relative abilities of the three species of Fe^{3+}-NTA to catalyze the reactions for initiation initiation of lipid peroxidation

	Fe^{3+}-NTA species			
Reaction in Scheme 2	(1:1:0)	(2:2:-2)	(2:2:-4)	Suggested findings
①	+++	++	–	Fig. 2
①+②*	+++	++	–	Fig. 4 (legend) and Fig. 5
①+②**	+++	++	–	Fig. 7(B) and (D)
③*	±	+	++	Fig. 1(●) and Fig. 4
③**	+	++	NE	Fig. 7(A) and (C)
④	+	++	++	Fig. 5
⑤	NE	–	NE	Fig. 6
①+②*+④	+++	++	+	Fig. 4 (legend)
①+②*+③+④	+++	++	+	Fig. 4

*L-OOH system, **H_2O_2 system, NE: not examined The reaction ② was faster catalyzed L-OOH-dependently than H_2O_2-dependently (from the results of Fig. 7(B) and (D)) The reaction ③ was faster catalyzed H_2O_2-dependently than L-OOH-dependently(from the results of Fig. 7(A) and (C)).

condition, and reactions ③ + ④ progressed under photo-irradiated condition. Reactions ① + ② did not occur either in photo-irradiated or photo-intercepted condition. At the conditions of pH 3 and pH 6, a reaction ③ only progressed under photo-intercepted condition. However, under photo-irradiated condition, reactions ① + ② mainly progressed in the presence of L-OOH and reactions ③ + ④ mainly progressed in the absence of L-OOH.

Recently, we reported that iron-chelate must bind to the membrane by coulombic attraction between the charged membrane and a chelate carrying the opposite net charge, and that among the iron-chelates tested, only iron(III)–NTA was an effective catalyst of peroxidation of membranes charged negatively and positively.[14] From these findings, we postulated that the unique catalytic capacity of the iron(III)–NTA complex can be explained by its existence in two forms, presumably (2:2:-2) and (2:2:-4) species, at neutral pH, each binding to oppositely charged membranes and initiating their peroxidation, which may be an important factor in its carcinogenicity. As the pH range of urine is broad (4.8.–7.5), three conformations of iron(III)–NTA are present depending on pH change of urine. The characteristics of iron(III)–NTA with three conformations, which have different abilities to induce lipid peroxidation by three different mechanisms observed in this study, also might cause its oxidative renal carcinogenesis.

References

[1] Bacon, B.R. and Britton, R.S. (1990) "The pathology of hepatic iron overload: a free radical-mediated process?", *Hepatology* **11**, 127–137.
[2] Rice-Evans, C., McCarthy, P., Hallinan, T., Green, N.A., Gor, J. and Diplock, A.T. (1989) "Iron overlord and the predisposition of cells to antioxidant cunsumption and peroxidative damage", *Free Radic. Res. Commun.* **7**, 307–313.
[3] Toyokuni, S. (1996) "Iron-induced carcinogenesis: the role of redox regulation", *Free Radic. Biol. Med.* **20**, 553–566.
[4] Okada, S. (1996) "Iron-induced tissue damage and cancer: the role of reactive oxygen species-free radicals", *Pathol. Int.* **46**, 311–332.
[5] Kawabata, T., Ma, Y., Yamador, I. and Okada, S. (1997) "Iron-induced apoptosis in mouse renal proximal tubules after an injection of a renal carcinogen, iron-nitrilotriacetate", *Carcinogenesis* **18**, 1389–1394.
[6] Shigenaga, M.K., Gimeno, C.J. and Ames, B.N. (1989) "Urinary 8-hydoxy-2′-deoxyguanosine as biological marker of *in vivo* oxidative DNA damage", *Proc. Natl Acad. Sci. USA* **86**, 9697–9701.
[7] Kasai, H. (1997) "Analysis of a form of oxidative DNA damage, 8-hydoxy-2′-deoxyguanosine, as a marker of cellular oxidative stress during carcinogenesis", *Mutat. Res.* **387**, 147–163.
[8] Okada, S., Minamiyama, Y., Hamazaki, S., Toyokuni, S. and Sotomatsu, A. (1993) "Glutathione cycle dependency of ferric nitrilotriacetate-induced lipid peroxidation in mouse proximal renal tubules", *Arch. Biochem. Biophys.* **301**, 138–142.
[9] Zainal, T.A., Weindruch, R., Szweda, L.I. and Oberley, T.D. (1999) "Localization of 4-hydroxy-2-nonenal-modified proteins in kidney following iron overload", *Free Radic. Biol. Med.* **26**, 1181–1193.
[10] Tanaka, T., Nishiyama, Y., Okada, K., Hirota, K., Matsui, M., Yodoi, J., Hiai, H. and Toyokuni, S. (1997) "Induction and nuclear translocation of thioredoxin by oxidative damage in the mouse kidney: independence of tubular necrosis and sulfhydryl depletion", *Lab. Investig.* **77**, 145–155.
[11] Toyokuni, S., Uchida, K., Okamoto, K., Hattori-Nakakuki, Y., Hiai, H. and Stadtman, E.R. (1994) "Fomation of 4-hydoroxy-2-nonenal-modified proteins in the renal proximal tubules of rats treated with a renal carcinogen, ferric nitrilotriacetate", *Proc. Natl Acad. Sci. USA* **91**, 2616–2620.
[12] Hamazaki, S., Okada, S., Li, J.-L., Toyokuni, S. and Midorikawa, O. (1989) "Oxygen reduction and lipid peroxidation by iron chelates with special reference to ferric nitrilotriacetate", *Arch. Biochem. Biophys.* **272**, 10–17.
[13] Fukuzawa, K., Fujii, T. and Mukai, K. (1991) "Peroxide-dependent and independent lipid peroxidations catalyzed by chelated iron", *Arch. Biochem. Biophys.* **290**, 489–496.
[14] Fukuzawa, K., Tokumura, A., Kogure, K., Iemura, M., Gondoh, N., Fujii, M., Ueno, S. and Shibata, A. (2001) "A comparative study of the ability of ferric nitrilotriacetate and other iron chelators to assist membrane lipid peroxidation by superoxide radicals", *Chem. Phys. Lipids* **110**, 69–84.
[15] Morel, I., Hamon-Bouer, C., Abalea, V., Cillard, P. and Cillard, J. (1997) "Comparison of oxidative damage of DNA and lipids in normal and tumor rat treated with ferric nitrilotriacetate", *Cancer Lett.* **119**, 31–36.
[16] Aruoma, O.I., Halliwell, B., Gajewski, E. and Dizdaroglu, M. (1989) "Damage to the bases in DNA induced by hydrogen peroxide and ferric ion chelates", *J. Biol. Chem.* **264**, 20509–20512.
[17] Nishida, Y. and Ito, S. (1995) "Structures and reactivities of several iron(III) complexes in the presence of hydrogen peroxide: relevance to induction of tissue damage caused by iron(III) chelates in rats", *Polyhedron* **14**, 2301–2308.
[18] Ogasawara, J. and Yokoi, H. (1996) "Studies on the complex formation of iron(III) with aminopolycarboxylic acids and related ligands by pH titration and magnetic susceptibility measurements", *Nihon Kagakkai-shi* **10**, 867–874.
[19] Gabricevic, M. and Crumbliss, A.L. (2003) "Kinetics and mechanism of iron(III)-nitrilotriacetate complex reactions with phosphate and acetohydroxamic acid", *Inorg. Chem.* **42**, 4098–4101.
[20] Buettner, G.R. (1993) "The pecking order of free radicals and antioxidants: lipid peroxidation, α-tocopherol, and ascorbate", *Arch. Biochem. Biophys.* **300**, 535–543.
[21] Van Dyke, B.R. and Saltman, P. (1996) "Hemoglobin: a mechanism for the generation of hydroxyl radicals", *Free Radic. Biol. Med.* **20**, 985–989.
[22] Smith, J.B., Cusumano, J.C. and Babbs, C.F. (1990) "Quantitative effects of iron chelators on hydroxyl radical production by the superoxide-driven Fenton reaction", *Free Radic. Res. Commun.* **8**, 101–106.
[23] Hard, G.C. (1998) "Mechanisms of chemically induced renal carcinogenesis in the laboratory rodent", *Toxicol. Pathol.* **26**, 104–112.
[24] Kawabata, T., Awai, M. and Kohno, M. (1986) "Generation of active oxygen species by iron nitrilotriacetate (Fe-NTA)", *Acta Med. Okayama* **40**, 163–173.
[25] Ozaki, M., Kawabata, T. and Awai, M. (1988) "Iron release from haemosiderin and production of iron-catalysed hydroxyl radicals *in vitro*", *Biochem. J.* **250**, 589–595.
[26] Kawabata, T., Okada, S., Akiyama, T. and Asaumi, A. (1992) "Generation of superoxide anion in Fe(III)-nta (nta = nitrilotriacetate) and system: an ESR study", *Chem. Lett.*, 2189–2192.
[27] Chao, C.C. and Aust, A.E. (1993) "Photochemical reduction of ferric iron by chelators results in DNA strand breaks", *Arch. Biochem. Biophys.* **300**, 544–550.
[28] Gay, C., Collins, J. and Gebicki, J.M. (1999) "Hydroperoxide assey with the ferric-xylenol orange complex", *Anal. Biochem.* **273**, 149–155.
[29] Fukuzawa, K., Iemura, M. and Tokumura, A. (1996) "Lipid peroxidation in egg phosphatidylcholine liposomes: comparative studies on the induction systems Fe^{2+}/ascorbate and Fe^{3+}-chelates/xanthine-xanthine oxidase", *Biol. Pharm. Bull.* **19**, 665–671.

[30] Mazur, H., Green, S., Saha, A. and Carleton, A. (1958) "Mechanism of release of ferritin iron *in vivo* by xanthine oxidase", *J. Clin. Investig.* **37**, 1809–1817.
[31] Eguchi, L.A. and Saltman, P. (1987) "Kinetics and mechanisms of metal reduction by hemoglobin. 1: reduction of iron(III) complexes", *Inorg. Chem.* **26**, 3665–3669.
[32] Hiat, R. and McColeman, C. (1987) "Catalysis of the reduction of hydroperoxides by triphenylphosphine", *Can. J. Chem.* **49**, 1712–1715.
[33] Webster, L.T. and Gabuzda, G.J. (1958) "Ammonium uptake by the extremities and brain in hepatic coma", *J. Clin. Investig.* **37**, 414–424.
[34] Saniabadi, A.R. (1994) "Photosensitizers and photochemical reactions", In: Nakashima, M., ed., *A Novel Photochemical Model for Thrombosis Research and Evaluation of Antithrombotic and Thrombolytic Agents* (Churchill Livingstone, Tokyo), pp 1–19.
[35] Niki, E. (1987) "Antioxidants in relation to lipid peroxidation", *Chem. Phys. Lipids* **44**, 227–253.